

# Bose-Einstein Condensation of Metastable Helium

F. Pereira Dos Santos, J. Léonard, Junmin Wang<sup>a</sup>, C. J. Barrelet,  
F. Perales<sup>b</sup>, E. Rasel<sup>c</sup>, C. S. Unnikrishnan<sup>d</sup>, M. Leduc, C. Cohen-Tannoudji  
Collège de France,

Laboratoire Kastler Brossel\*, Département de Physique, Ecole Normale Supérieure,  
24 rue Lhomond, 75231 Paris Cedex 05, France  
(February 19, 2019)

We have observed a Bose-Einstein Condensate in a dilute gas of  $^4\text{He}$  in the  $2^3S_1$  metastable state. We find a critical temperature of  $(4.7 \pm 0.5) \mu\text{K}$  and a typical number of atoms at the threshold of  $8 \times 10^6$ . The maximum number of atoms in our condensate is about  $5 \times 10^5$ . An approximate value for the scattering length  $a = (16 \pm 8) \text{ nm}$  is measured. The elastic collision rate is then estimated to be about  $5 \times 10^4 \text{ s}^{-1}$ , indicating that we are deeply in the hydrodynamic regime. The typical decay time of the condensate is 2 s which places an upper bound on the rate constants for 2-body and 3-body inelastic collisions.

PACS numbers: 03.75.Fi, 05.30.Jp, 32.80.Pj

Bose-Einstein condensation (BEC) of dilute atomic gases was first observed in alkali atoms in 1995 and then, a few years later in atomic hydrogen. Since then, the field has developed in a spectacular way both experimentally and theoretically [1]. So far only condensates with atoms in their electronic ground state have been produced.

Several laboratories are currently involved in the search for BEC of atoms in an excited state, namely noble gases in an excited metastable state. Helium in its triplet metastable  $2^3S_1$  state ( $^4\text{He}^*$ ) is of particular interest. The first advantage of  $^4\text{He}^*$  is its large internal energy (19.8 eV). It allows for a very efficient detection of the atom by ionization after collision with another atom or a surface, which can be of interest for atomic lithography [2,3]. Second, helium is a relatively simple atom which allows for quasi-exact calculations that are useful in metrological applications. Third, mixtures of  $^3\text{He}$  and  $^4\text{He}$  can be used to study quantum degenerate mixtures of bosons and fermions. Finally, Penning ionization collisions between  $^4\text{He}^*$  atoms raise an interesting question related to BEC. Theoretical calculations [4,5] predict the inhibition of the Penning ionization rate of spin polarized atoms, due to spin selection rules. Is this inhibition large enough to reach the condensation threshold?

The present article describes the observation of BEC of  $^4\text{He}^*$  atoms. Similar results have also been obtained at IOTA, Orsay [6]. The two experiments differ by their detection methods. The Orsay group detects the atoms falling on a microchannel plate, whereas we use an optical absorption imaging of the atomic cloud on a CCD camera. The two experiments give therefore different and complementary information on the physics of BEC in  $^4\text{He}^*$ .

The first step of our experiment is the efficient loading of a magneto-optical trap (MOT). The experimental set-up is described in detail in [7]. A discharge atomic source ensures a high flux of triplet metastable atoms of  $10^{14}$  atoms/second/steradian, with a mean velocity of about

1000 m/s. The atomic beam is collimated [8] and Zeeman slowed by laser light at 1083 nm ( $2^3S_1$ - $2^3P_2$  transition). A narrow frequency band master oscillator (DBR diode laser) injects a Yb-doped fiber amplifier with an output power of 500 mW. Using this set-up, it is possible to trap  $\sim 8 \times 10^8$  atoms in the MOT at a temperature of 1 mK.

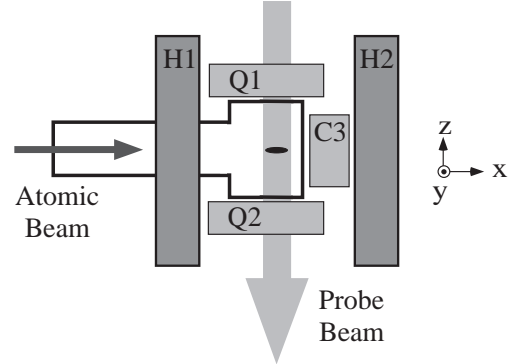


FIG. 1. Top view of the magnetic trap. Coils  $Q_1$  and  $Q_2$  produce a quadrupole field used for the MOT. Combined with a third coil  $C_3$ , they produce a magnetic Ioffe- Pritchard trap. Helmholtz coils  $H_1$  and  $H_2$  compensate the field bias. The probe beam used for optical detection is perpendicular to the longitudinal axis of the trap.

$^4\text{He}^*$  atoms are confined at the center of a small ( $4 \times 4 \times 5 \text{ cm}$ ) quartz cell. All coils are external to the cell (see Fig.1). The coils  $Q_1$  and  $Q_2$  (144 turns and 7 cm diameter) combined with the coil  $C_3$  (108 turns and 4 cm diameter) produce an anisotropic magnetic Ioffe-Pritchard trap. Two additional Helmholtz coils reduce the field bias, in order to increase the radial confinement of the trap. A current of 45 A in all the coils produces a 4.2 G bias field, radial gradients of 280 G/cm and an axial curvature of 200 G/cm<sup>2</sup>. These values correspond to trapping frequencies of 115 Hz in the axial and 1090 Hz in the radial directions. The current in the coils can

be switched off in 200  $\mu\text{s}$ .

The second step of the experiment is the loading of the magnetic trap. After switching off the MOT field, the cloud is further cooled down to about 300  $\mu\text{K}$  during a 1 ms optical molasses phase. To increase the transfer efficiency from the molasses to the magnetic trap, the atoms are optically pumped by a circularly polarized laser pulse.  $3 \times 10^8$  atoms are loaded in the magnetic trap. The lifetime of the atomic cloud in the magnetic trap is about 35 seconds, its temperature is 1.2 mK after compression and bias compensation.

The last step of the experiment consists of evaporative cooling performed by radio frequency (RF) induced spin flips. The frequency is ramped down from 160 MHz to around 12 MHz in 15 seconds. After evaporation, the trap is switched off and the cloud released from the trap is probed by absorption imaging on a CCD camera whose quantum efficiency is 1.5% at 1083 nm.

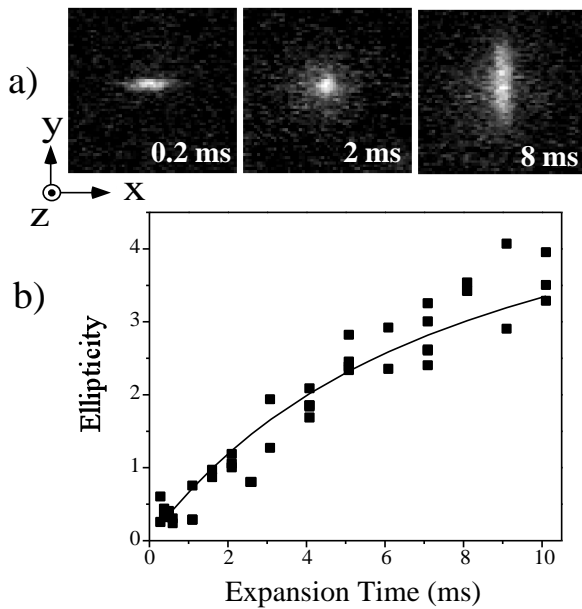


FIG. 2. a) Time-of-flight absorption images ( $1.4 \times 1.4$  mm) after an expansion time of 0.2, 2 and 8 ms; b) Ellipticity of the condensate for increasing expansion times. The solid line is the theoretical prediction without any adjustable parameters. The inversion of ellipticity is characteristic of the behaviour of an expanding condensate.

When the RF frequency of the evaporation is ramped down to a final frequency below 13 MHz, a narrow structure appears on the absorption image which we identify as a condensate. The strongest evidence for the presence of the condensate is the evolution of the shape of the atomic cloud when released from the trap in the time-of-flight (TOF) measurement. As the expansion time is increased, the anisotropy of the structure increases and the ellipticity of the cloud undergoes an inversion (see Fig.2 a). This observation is a consequence of the mean-field interaction between atoms in the condensate [9]. The

theoretical prediction containing no adjustable parameters agrees well with our measurements (see Fig.2 b).

The spatial distribution of the absorption pictures is fitted with the sum of two functions, one for the condensate and one for the thermal cloud (see insert in fig. 3). The function for the condensate is an integration along the z-axis of a paraboloidal distribution. It describes in the Thomas-Fermi limit the equilibrium density profile of the condensate within the harmonic trap [10]. The function for the thermal cloud is a  $g_2$  function valid for a bosonic gas close to the transition where the chemical potential  $\mu$  is an adjustable parameter [1]. From the fit, we extract the ratio between the number of atoms in the condensate,  $N_0$ , and the total number of atoms,  $N$ . Plotting  $N_0/N$  versus the temperature  $T$  (Fig.3) gives the value of the critical temperature  $T_c = 4.7 \pm 0.5 \mu\text{K}$ , which is confirmed by a TOF measurement performed on a thermal cloud just above the transition.

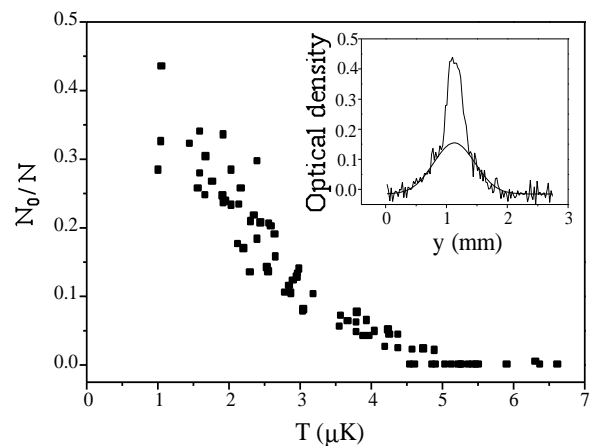


FIG. 3. Condensed fraction  $N_0/N$  versus  $T$ . The inset shows a 1D profile of an absorption image, displaying a bimodal structure, composed of a condensate and a thermal component, which is characteristic of the bosonic gas below  $T_c$ . The thermal component was fitted for clarity.

The results presented until now are based only on measured sizes of the clouds and on relative numbers like  $N_0/N$  which do not require absolute calibration of the optical detection. The procedure described previously for measures of ellipticity and critical temperature is inappropriate for absolute measures of  $N$  and  $N_0$ . Instead, the current is switched off in two steps: first, in the Helmholtz coils, then after a delay of 10 ms, in the 3 coils  $Q_1$ ,  $Q_2$  and  $C_3$ , whereas the current in all five coils was switched off simultaneously for the measurements above. Then, we take an absorption image with an exposure time of  $T_{exp} = 200 \mu\text{s}$  after a TOF time of 5 ms. This procedure minimizes the effects of eddy currents of the Helmholtz coils which last several milliseconds, Zeeman shifting the atomic resonance with respect to the probe beam frequency [11].

There are two other obvious sources of sensitivity losses. First, the width of the absorption lineshape was measured to be twice the natural linewidth, which reduces the absorption cross-section by a factor 2. Second, the probe beam propagates perpendicularly to the axis of the Ioffe-Pritchard trap (see Fig.1) along which atoms are polarized. It is therefore necessary to take into account the Clebsch-Gordan coefficients of the various Zeeman optical transitions excited by the probe beam. A simple calculation gives an extra loss by a factor 9/5. Finally, there is another source of losses which is specific to  $^4\text{He}^*$  when optically detected and particularly important at the high densities obtained in our experiment. The metastable atoms have a huge Penning ionization cross-section in the presence of resonant light, so that losses can accumulate during the probe pulse at large densities. Unfortunately, probing at low intensity is no more possible if  $T_{exp}$  is made shorter because of the low efficiency of the CCD camera. This long exposure time also increases the acceleration of the atoms due to radiation pressure which pushes them out of resonance [12]. In the present stage of the experiment, it is difficult to give a quantitative description of the combined effect of these phenomena. So, we prefer to avoid them by waiting an expansion time before probing, typically 5 ms, long enough for reducing atomic densities to sufficiently small values. Indeed, we observe that the measured number of atoms is an increasing function of the expansion time reaching a plateau after 5-6 ms. After the corrections mentioned above, the total number of atoms  $N_c$  at the threshold is measured to be  $5 \times 10^6$  atoms with an accuracy of about 50%.

$N_c$  can also be estimated from  $N_c = 1.202(k_B T_c / \hbar \omega)^3$ , where  $\omega$  is the geometrical average of the frequencies of the trap [13]. We deduce  $N_c = 8.2 \times 10^6$  atoms with an uncertainty of about 30% compatible with the previous one. Because it is easier to trace down the error on  $N_c$  when derived from  $T_c$ , we arbitrarily choose this value of  $N_c$  to estimate the scattering length  $a$ . Also, assuming that the transition occurs at a phase space density equal to  $n(0)\lambda_{dB}^3 = 2.612$ , where  $\lambda_{dB}$  is the de Broglie wavelength, we can also derive the density at the center of the trap  $n(0) = (3.8 \pm 0.7) \times 10^{13}$  atoms/cm<sup>3</sup> at the transition.

Within the Thomas-Fermi approximation, one can extract the chemical potential  $\mu$  from the size of the condensate [10]. As the optical detection around the transition has been calibrated, one can now deduce the absolute number of atom  $N_0$  below the transition. Typical values of  $\mu = 1.4 \times 10^{-29}$  J and  $N_0 = (4 \pm 1.5) \times 10^5$  are obtained with condensates prepared at temperatures ranging from 1.2  $\mu$ K to 3  $\mu$ K. Finally an estimation of the scattering length  $a$  can be given using  $a = \sigma / 15 N_0 \times (2\mu / \hbar \omega)^{5/2}$ , where  $\sigma = (\hbar / m \omega)^{1/2}$  is the characteristic size of the ground state of the trap. We find  $a = (16 \pm 8)$  nm which is compatible with the value given by recent theoretical

works [4,14]. The error is mainly due to the uncertainty on the number of atoms. Knowing the scattering length  $a$ , the density at the center of the trap  $n(0)$  and the critical temperature  $T_c$ , we obtain a rate of elastic collisions  $\simeq 5 \times 10^4$  s<sup>-1</sup> at the center of the cloud near threshold. The mean time between elastic collisions being shorter than the oscillation periods in the trap, we thus enter in the hydrodynamic regime, an interesting feature for a gas above  $T_c$  [15–17].

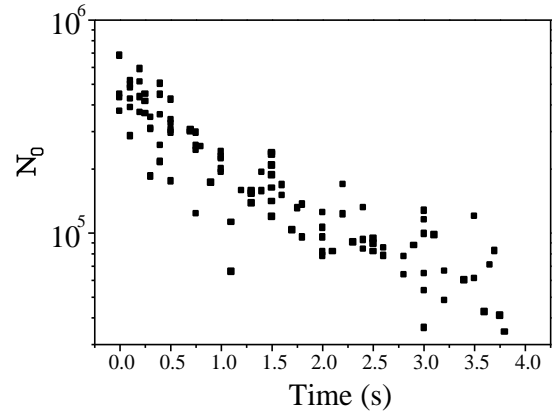


FIG. 4. Decay of the condensate. This measurement was performed with an RF shield at 12.3 MHz.

Fig.4 shows the evolution of the number of atoms in the condensate versus the trapping time. The typical lifetime is about 2 s. In the present stage of the experiment, it is not possible to discriminate between 2-body or 3-body decay. However, assuming that only 2-body collisions lead to losses in the condensate, we can place an upper bound on the collision rate constant  $G$  between spin polarized  $^4\text{He}^*$  atoms, which is predicted to be inhibited by a factor  $10^4$  compared with the rate constant for Penning ionization collisions between unpolarized atoms [4,5]. The evolution equation of the number of atoms  $\dot{N}(t) = -G \int n^2(\mathbf{r}) d^3\mathbf{r}$ , integrated on the whole condensate in the Thomas-Fermi approximation, gives the evolution of the number of atoms  $N_0$  in the condensate. A fit leads to  $G \leq (4.2 \pm 0.6) \times 10^{-14}$  cm<sup>3</sup>/s, which corresponds to a reduction factor larger than  $2 \times 10^3$ , much larger than the previously measured ones [18,19].

If one assumes now that 3-body collisions are responsible for the decay of  $N_0$ , one can as well give an upper bound for the rate constant  $L$  defined by  $\dot{N}(t) = -L \int n^3(\mathbf{r}) d^3\mathbf{r}$ . Fitting our data gives  $L \leq (2.8 \pm 0.2) \times 10^{-27}$  cm<sup>6</sup>/s. This value can be compared to theoretical predictions [20,21]: for example, our upper limit is compatible with [20] who finds  $L = 3.9 \hbar a^4 / 2m = 2 \times 10^{-27}$  cm<sup>6</sup>/s.

In conclusion, this article shows the evidence for the formation of a BEC of helium atoms in the metastable state  $2^3S_1$ . Our optical detection method allows to clearly visualize the change of anisotropy of the con-

densate during the expansion. The design of our magnetic trap provides relatively high densities of atoms at the threshold of condensation. Combined with the large value that we find for the scattering length, this results in very large rates of elastic collisions : the cold gas is in the hydrodynamic regime, which offers interesting features in the context of BEC. Our results concerning the losses due to inelastic collisions show that the spin polarization does inhibit the Penning ionization collisions between 2 metastable helium atoms by more than 3 orders of magnitude, as theoretically predicted. Improvement can be brought to the experiment that will hopefully lead to more accurate results on elastic and inelastic collisions. Then we plan to further exploit the original characteristics of this new born condensate of atoms in an excited state.

**Acknowledgments:** The authors wish to thank J. Dalibard, C. Salomon, D. Guéry-Odelin and Y. Castin for helpful discussions and careful reading of the manuscript. We thank the IOTA group in Orsay for communicating their preliminary results as soon as they were obtained, which was a great stimulation for our group achieving helium BEC 8 days later. Also, we thank M. Roux for the loan of the Hamamatsu CCD camera (C4880-30) with which the BEC was first detected in our group. C.J.B. acknowledges the support from the Schweizerische Studienstiftung.

<sup>a</sup> Permanent address: Institute of Opto-Electronics, Shanxi University, 36 Wucheng Road, Taiyuan, Shanxi 030006, China.

<sup>b</sup> Permanent address: Laboratoire de Physique des Lasers, UMR 7538 du CNRS, Université Paris Nord, Avenue J.B. Clément, 93430 Villetaneuse, France.

<sup>c</sup> Present address : Universität Hannover, Welfengarten 1, D-30167 Hannover, Germany.

<sup>d</sup> Permanent address : TIFR, Homi Bhabha Road, Mumbai 400005, India.

\* Unité de Recherche de l'Ecole Normale Supérieure et de l'Université Pierre et Marie Curie, associée au CNRS (UMR 8552).

- 
- [1] For an overview on the subject, see for example: the Proceedings of the International School of Physics "Enrico Fermi" Course CXL, M. Inguscio, S. Stringari and C. E. Wieman (Eds), IOS Press, Amsterdam (1999)
- [2] A. Bard, K. K. Berggren, J. L. Wilbur, J. D. Gillaspay, S. L. Rolston, J. J. McClelland, W. D. Phillips, M. Prentiss and G. M. Whitesides, *J. Vac. Sc. Technol. B* **15**, 1805 (1997).

- [3] S. Nowak, T. Pfau and J. Mlynek, *Appl. Phys. B* **63**, 203 (1996)
- [4] G. V. Shlyapnikov, J. T. M. Walraven, U. M. Rahmanov and M. W. Reynolds, *Phys. Rev. Lett.* **73**, 3247 (1994); P. O. Fedichev, M. W. Reynolds, U. M. Rahmanov and G. V. Shlyapnikov, *Phys. Rev. A* **53**, 1447 (1996)
- [5] V. Venturi, I. B. Whittingham, P. J. Leo and G. Peach, *Phys. Rev. A* **60**, 4635 (1999)
- [6] IOTA group at Orsay, to appear in *Science*
- [7] F. Pereira Dos Santos, F. Perales, J. Léonard, A. Sinatra, Junmin Wang, F. S. Pavone, E. Rasel, C. S. Unnikrishnan and M. Leduc, accepted for publication in *Eur. Phys. J. A*
- [8] E. Rasel, F. Pereira Dos Santos, F. S. Pavone, F. Perales, C. S. Unnikrishnan and M. Leduc, *Eur. Phys. J. D* **7**, 311 (1999)
- [9] Y. Castin and R. Dum, *Phys. Rev. Lett.* **77**, 5315 (1996)
- [10] See for example, F. Dalfovo, S. Giorgini, L. P. Pitaevskii and S. Stringari, *Rev. Mod. Phys.* **71**, 463 (1999)
- [11] Because of the large size of the Helmholtz coils, one can however neglect the spatial gradients of magnetic fields corresponding eddy currents. The measurement of the sizes and of the ratios  $N_0/N$  is thus not affected by these remaining magnetic fields.
- [12] Actually, we use a standing wave made of two independent opposite beams in order to reduce the effect of radiation pressure.
- [13] This formula is only valid in the case of an ideal bosonic gas and does not make any further assumption. Effects due to mean field have been calculated for an harmonic trap [22] and effects due to quantum correlations have been calculated in a box [23]. The shift of the critical temperature  $T_c$  can be quite large ( $\delta T_c/T_c \simeq 15\%$ ) for both of these effects due to the large value of the scattering length  $a$  but have opposite signs. It would be interesting to study them both in more detail for an harmonic trap.
- [14] V. Venturi and I. B. Whittingham, *Phys. Rev. A* **61**, 060703-1 (2000); V. Venturi, I. B. Whittingham and J.F. Babb, preprint arXiv:physics/0011072
- [15] D. M. Stamper-Kurn, H.-J. Miesner, S. Inouye, M. R. Andrews and W. Ketterle, *Phys. Rev. Lett.* **81**, 500 (1998)
- [16] A. Griffin, Wen-Chin Wu and S. Stringari, *Phys. Rev. Lett.* **78**, 1838 (1997)
- [17] D. Guéry-Odelin, F. Zambelli, J. Dalibard and S. Stringari, *Phys. Rev. A* **60**, 4851 (1999)
- [18] N. Herschbach, P. J. J. Tol, W. Hogervorst and W. Vassen, *Phys. Rev. A* **61**, 050702 (2000)
- [19] S. Nowak, A. Browaeys, J. Poupard, A. Robert, S. Nowak, D. Boiron, C. Westbrook and A. Aspect, *Appl. Phys. B* **70**, 455 (2000)
- [20] P. O. Fedichev, M. W. Reynolds and G. V. Shlyapnikov, *Phys. Rev. Lett.* **77**, 2921 (1996)
- [21] B. P. Esry, C. H. Greene and J. P. Burke, *Phys. Rev. Lett.* **83**, 1751 (1999)
- [22] S. Giorgini, L. P. Pitaevskii and S. Stringari, *Phys. Rev. A* **54**, R4633 (1996)
- [23] M. Holzmann and W. Krauth, *Phys. Rev. Lett.* **83**, 2687 (1999)